Chapter

Thermally Activated Delayed Fluorescence (TADF) Compounds as Photocatalyst in Organic Synthesis: A Metal-Free Greener Approach

Suresh Rajamanickam and Bhisma K. Patel

Abstract

Thermally activated delayed fluorescent (TADF) molecules undergo efficient intersystem crossing (ISC) and reverse intersystem crossing (RISC) processes, making them as third-generation emitters in organic light-emitting diodes (OLEDs), photo-dynamic therapy (PDT) and time-resolved luminescence imaging. Apart from these applications, recently, TADF molecules have been used extensively as photocatalysts in light-mediated synthesis. In general, highly expensive complexes of Rh, Ir, Ru and organic dyes (Eosin Y, Rose Bengal, 9-mesityl-10-methylacridinium perchlorate [Acr-Mes]$^+$ClO$_4^-$) are commonly used in the photocatalysis process. Organic-TADF based molecules help to avoid these costly metal catalysts and frequently used organic dyes, making the reaction economical and greener. This chapter will briefly summarize the photocatalytic properties of organic-TADF compounds in organic synthesis.

Keywords: thermally activated delayed fluorescence (TADF), photocatalysis, 4CzIPN, organo photoredox catalysis, radical chemistry, single electron transfer (SET), halogen atom transfer (XAT), cross dehydrogenative coupling (CDC), Minisci reaction, cyclopropanation, cyclization reaction, ring opening reaction, deuteration reaction, hydroformylation reaction

1. Introduction

The term 'photocatalysis' is derived from the concepts of photochemistry. Previously, ultraviolet (UV) irradiation was commonly applied in classical photochemical reactions. The use of high energy ultraviolet light has selectivity issues and requires a designer reaction setup. However, the recent photochemical reaction uses low energy and selective wavelength of visible light from Light-Emitting Diodes (LED). Due to low energy usage, modern photochemical reactions are highly selective. In general, visible light has low absorptivity, so it can not drive the organic reaction competently. A secondary substrate, usually a photocatalyst is introduced to enhance the light

absorptivity. This photocatalyst absorbs visible light and provides stable and long photoexcited states, which induces the substrates or reagents to participate in the chemical reaction. The photoexcited catalyst either donates or removes a single electron from the reacting partners, which triggers further reaction *via* oxidative or reductive quenching. The current need of modern organic chemistry is the effective utilization of raw materials, energy resources. Further, elimination of waste, toxic, hazardous solvents, reagents and replacement of expensive and less efficient processes are the basic tenets of Green Chemistry. In this regard, visible-light assisted photo-catalyzed reactions provides a smooth pavement for sustainable chemical synthesis. In addition, the visible-light assisted photo-catalyzed reaction received much attention in the synthetic community due to the simplicity of reaction setup and broad applicability to various reactions. However, most visible light-mediated reactions use expensive metal-based Ru or Ir based photoredox complexes making the process economically unviable. Nevertheless, the use of bench-stable inexpensive Thermally Activated Delayed Fluorescence (TADF) organic material as photocatalysts obviate many of the problems.

Polish physicist Aleksander Jabłoński studied the molecular absorbance and emission of light. He developed the famous Jablonski diagram to explain the spectra and kinetics of fluorescence and phosphorescence. This diagram illustrates the excited states energy level of a molecule and their radiative and non-radiative transitions. A typical Jablonski diagram is shown in **Figure 1a**. Under appropriate light irradiation, the molecules excite to an excited singlet state (Sn), and then the excitons migrate to the lowest excited singlet state (S_1) *via* internal conversion (IC). The lowest excited singlet state (S_1) excitons subsequently migrate from the S_1 state to the ground state
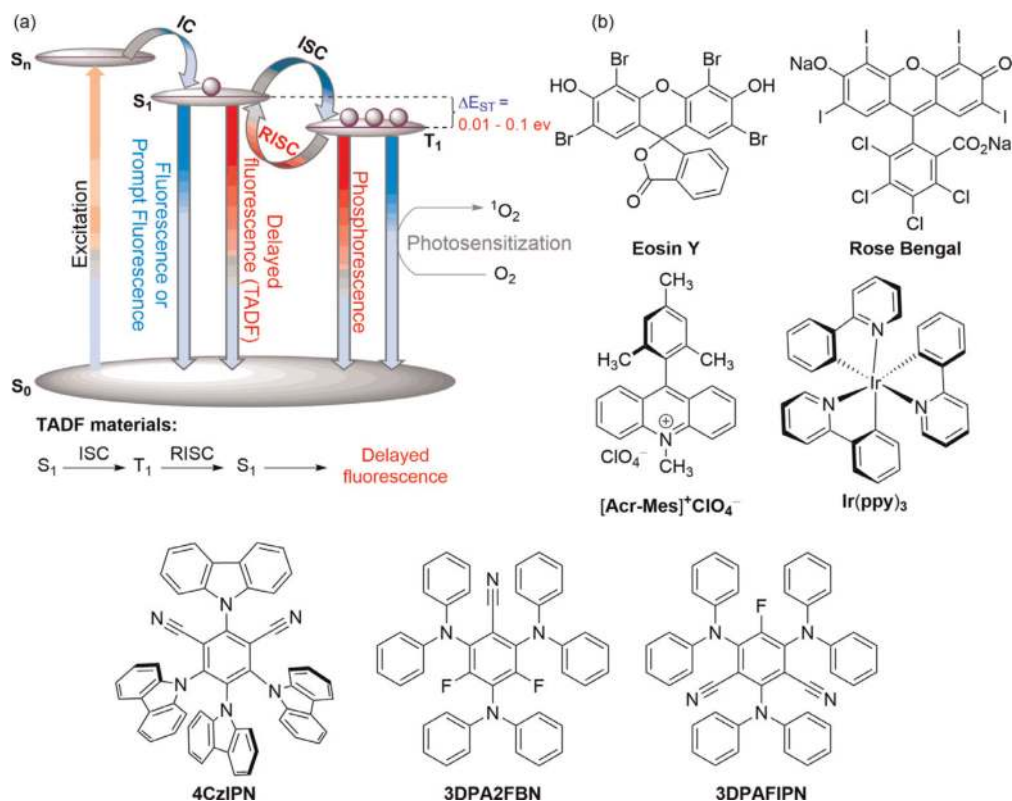

Figure 1.
Simplified Perrin-Jablonski diagram and commonly used TADF motif in photocatalysis.

(S_0) by releasing radiative light energy. This process is known as fluorescence or prompt fluorescence. Meanwhile, the singlet state excitons (S_1) can further migrate to the lowest triplet excited state (T_1) through intersystem crossing (ISC), which can undergo a radiative decay transition process from the lowest triplet excited state (T_1) to the ground state (S_0), ($T_1 \rightarrow S_0$ transition) which is termed as phosphorescence.

Followed by Jabłoński, French physicists Jean Baptist Perrin, the winner of 1926 Nobel Prize in Physics, and his son Francis Perrin rationalized a third type of radiative transition known as delayed fluorescence. This occurs when a molecule in the lowest triplet excited state (T_1) transitions to the lowest excited singlet state (S_1) *via* reverse intersystem crossing (RISC) followed by a radiative transition to the ground state (S_0). The reverse intersystem crossing (RISC) from T_1 to S_1 is only possible when the molecule has a very small singlet-triplet energy gap ΔE_{ST} (upto < 0.6 ev) between the lowest-lying singlet S_1 and triplet excited states T_1. When the ΔE_{ST} is very small, the environment heat helps to achieve the reverse intersystem crossing ($T_1 \rightarrow S_1$), resulting in delayed fluorescence. The overall process is termed as Thermally Activated Delayed Fluorescent (TADF). These TADF molecules have huge applications in the third-generation Organic Light-Emitting Diode (OLED) display technology. According to Transparency Market Research, the global OLED displays market is expected to reach $100 billion by 2030 from $4.9 billion in 2012. Recently, the TADF process is also incorporated in the Jablonski diagram and the diagram is termed as Perrin-Jablonski diagram.

The TADF proceeds *via* the result of multiple cycles between intersystem crossing (ISC) from S_1 to T_1 and the reverse intersystem crossing (RISC) from T_1 to S_1. So a delayed fluorescence is observed after the short-lived fluorescence. TADF emission is identical in wavelength to prompt fluorescence, but it occurs on a longer timescale. The emission lifetime of fluorescence or prompt fluorescence is shorter (nanosecond scale). On the other hand, the delayed fluorescence has a longer emission lifetime (microsecond or even millisecond scale).

Eosin Y is the first organic compound identified to show Thermally Activated Delayed Fluorescence (TADF) property. This inexpensive organic dye is widely used in photocatalysis (PC) due to its moderate redox potentials (in 1:1 ratio of acetonitrile and water ratio the ground oxidation and reduction potentials of Eosin Y are E_{ox} = 0.78 V and E_{red} = −1.06 V respectively. The excited state reduction and oxidation potentials are E_{ox}* = −1.11 V and Er_{ed}* = 0.83 V) and visible region absorption (λ_{abs} = 520 nm in MeOH). Followed by Eosin Y, other organic TADF molecules such as Rose Bengal, 9-mesityl-10-methylacridinium perchlorate [Acr-Mes]$^+$ClO$_4{}^-$ and polypyridyl metal complexes Ir(ppy)$_3$, (Ir[dF(CF$_3$)ppy]$_2$(dtbpy))PF$_6$ and [Ru(bpy)$_3$] (PF$_6$)$_2$) were extensively studied in photocatalysis process (**Figure 1**).

In 2012, Adachi group prepared a conformationally twisted electron-donor and acceptor TADF material, 2,4,5,6-tetra(carbazol-9-yl)benzene-1,3-dicarbonitrile (4CzIPN) by single-step reaction between 2,4,5,6-tetrafluoroisophthalonitrile and carbazole *via* nucleophilic aromatic substitution (S$_N$Ar) reaction (**Figure 2**) [1]. This molecule has a very small energy gap (ΔE_{ST} = 0.08 eV in toluene) between S_1 and T_1 levels. This small energy difference allows reverse intersystem crossing (RISC) from T_1 to S_1 to qualify it as a TADF molecule [1]. 4CzIPN is a poor single-electron oxidant or reductant in the ground states. On the other hand, it is a potent single electron transfer reagent in the excited states under visible-light irradiation. This TADF molecule has high photoluminescence quantum yield (94.6%) and a long lifetime at an excited state (5.1 μs). One of the primary advantages of 4CzIPN is its low synthetic cost [2].
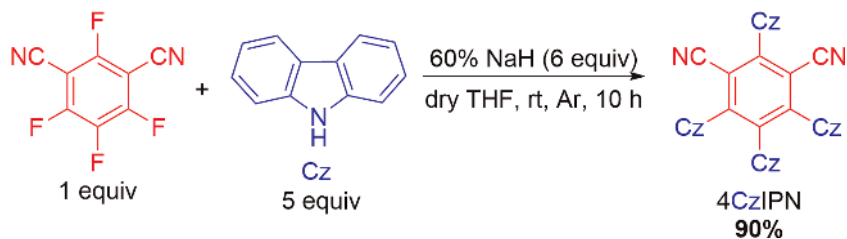
Figure 2.
Synthesis of 2,4,5,6-tetra(carbazol-9-yl)benzene-1,3-dicarbonitrile (4CzIPN).
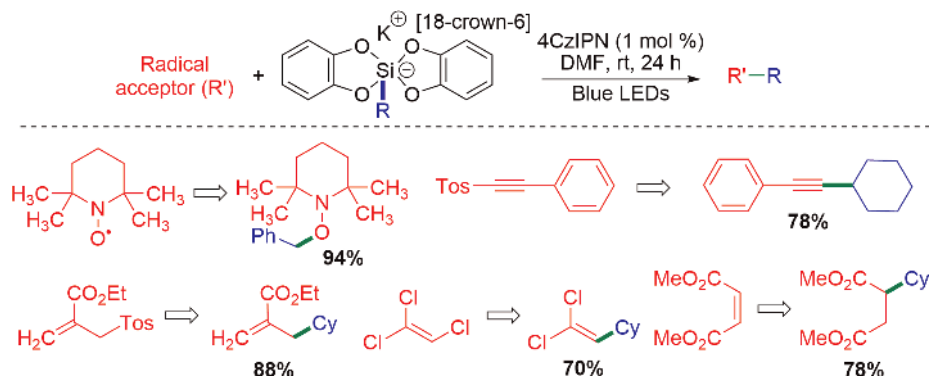

Figure 3.
4CzIPN-catalyzed radical functionalization of silicates with various radical acceptors.

In 2016, Ollivier and Fensterbank group used 4CzIPN as a photocatalyst for an organic transformation [3]. Under blue LEDs irradiation, 4CzIPN undergo photoexcitation, the photoexcited 4CzIPN* generated benzyl radical from benzyl *bis* (caecholato)silicates, the generated radical is trapped by (2,2,6,6-tetramethyl-piperidin-1-yl)oxyl (TEMPO) (**Figure 3**). The author further extended the scope of this methodology for the preparation of alkynylation, vinylation and Giese-type products by treating alkylsilicates with a variety of radical acceptors (**Figure 3**). This work open-up a new window for many organic transformations using 4CzIPN as an economically cheaper, greener organo photoredox catalyst.

Followed by Ollivier and Fensterbank radical-mediated synthesis [3], various organic transformations were documented using 4CzIPN as a photocatalyst under the irradiation of visible light or blue LEDs. Besides this, many reactions were reported using 4CzIPN in combination with a transition metal. This chapter excludes transition metal assisted (synergic catalysis) synthesis and mainly focuses on 4CzIPN as an independent photocatalyst without any transition metals.

2. Cyclopropanation reactions

In 2018, a group of Gutierrez and Molander demonstrated a redox-neutral photocatalytic cyclopropanation of olefins with triethylammonium *bis*(catecholato) iodomethylsilicate using a combination of 4CzIPN and blue LEDs light. Triethylammonium *bis*(catecholato)iodomethylsilicate serve as an iodomethyl radical precursor (**Figure 4**) [4].

From mechanistic aspects, the photocatalytically generated halomethyl radical is trapped by the alkene and generate a stable tertiary radical. This radical accepts a
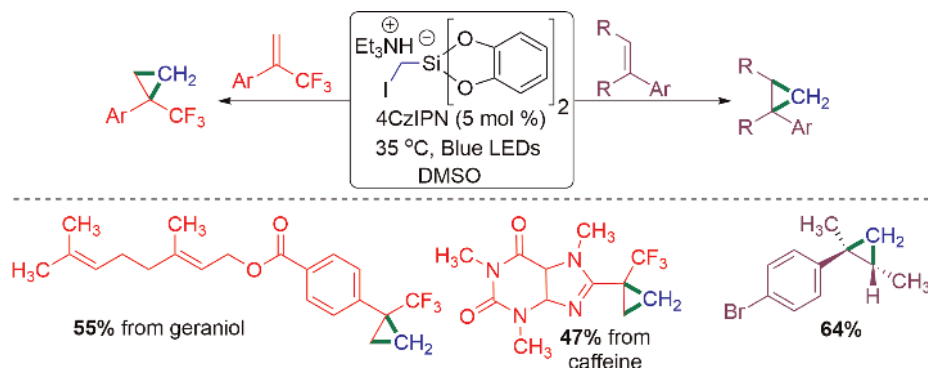
Figure 4.
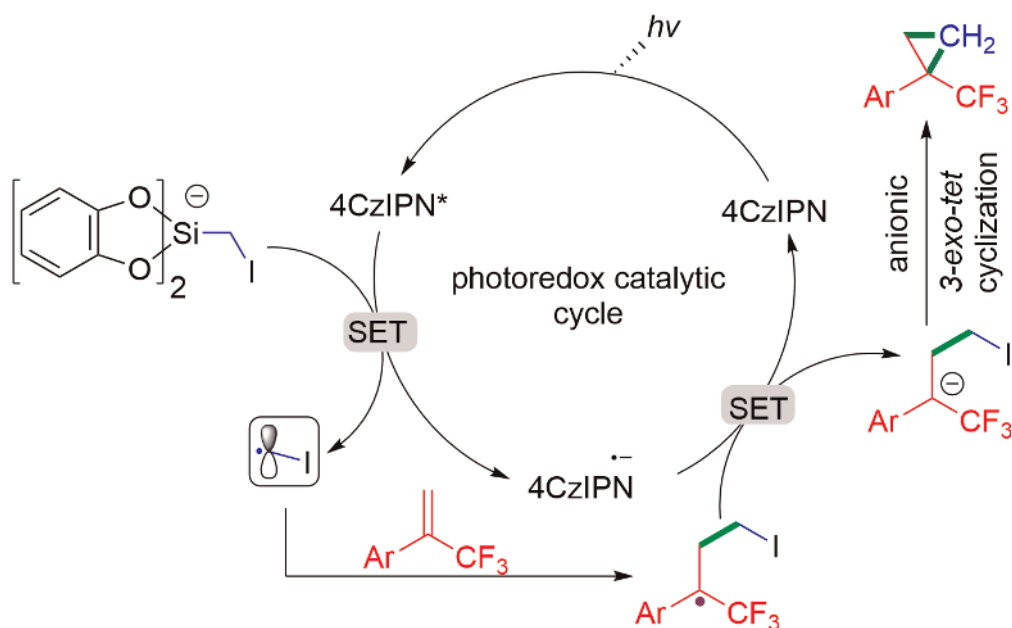*4CzIPN-catalyzed cyclopropanation of alkene using iodomethylsilicate.*

Figure 5.
4CzIPN-catalyzed cyclopropanation of alkene using iodomethylsilicate.

single electron from the 4CzIPN$^{•-}$, to form an anion and regenerate the catalyst. It underwent an anionic *3-exo-tet* ring closure that leads to a cycopropylation product. With the support of both computational and control experiments performed, the authors concluded that the reaction proceeds *via* an anionic *3-exo-tet* ring closure (**Figure 5**) [4].

In the same year, the Molander group further extended their aforementioned cyclopropanation methodology [4] to the homoallylic tosylates system (**Figure 6**) [5]. In their previous report, the leaving group (iodo) is attached to the radical precursor motif itself [4]. In their follow-up work, the Molander group incorporated the leaving group into the alkene core. They treated three different alkyl radical precursors such as *bis*(catecholato)alkylsilicates, alkyltrifluoroborates and 4-alkyl dihydropyridines, with an array of linear homoallylic tosylates systems [5]. All leads to 1,1-disubstituted cyclopropanes derivatives in moderate to good yields *via in-situ* generated anionic cyclization (**Figure 6**). The classical electrophilic carbenoid Simmons-Smith
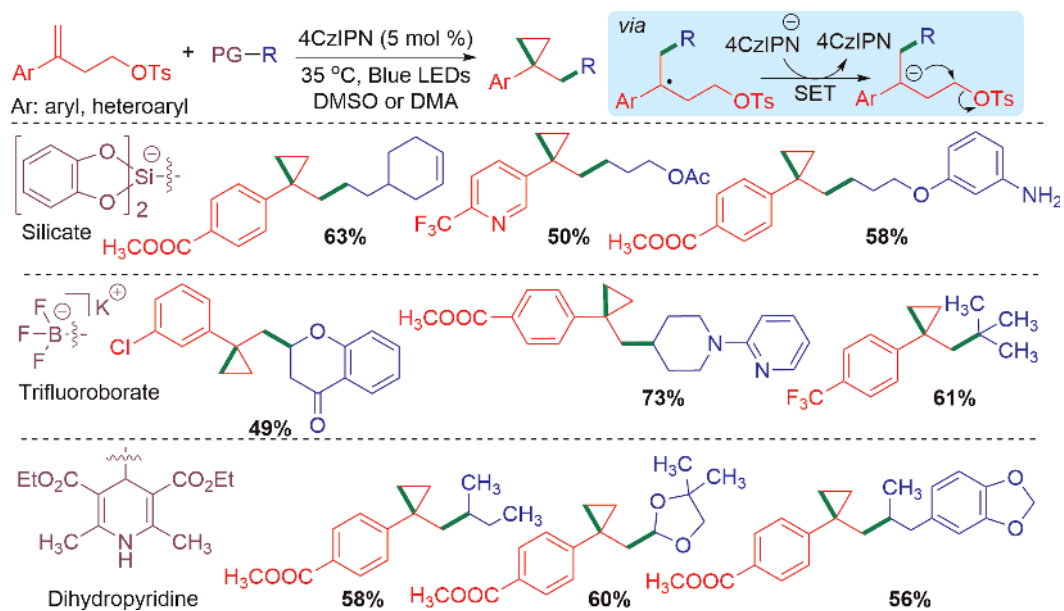
Figure 6.
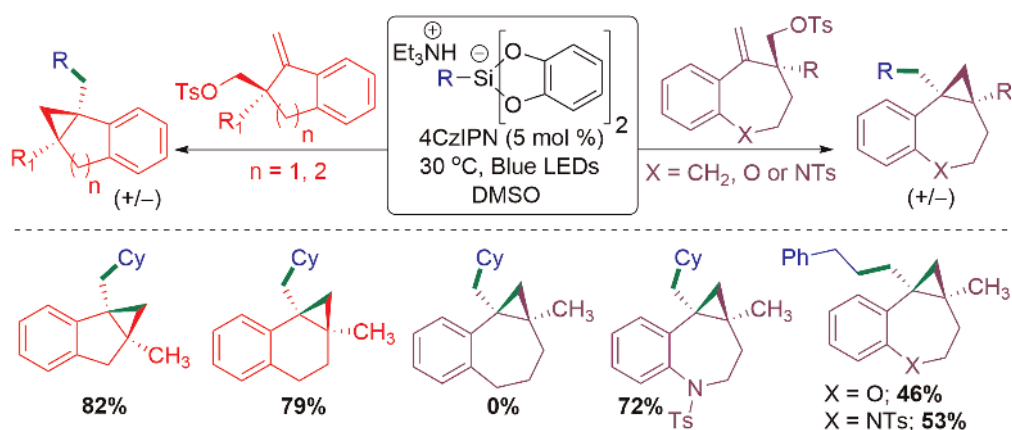*4CzIPN-catalyzed cyclopropanation of linear homoallylic tosylates using alkyl radical precursors.*

Figure 7.
4CzIPN-catalyzed cyclopropanation of exocyclic homoallylic tosylates using bis(catecholato)alkylsilicates.

cyclopropanation reaction is incompatible for Lewis basic heterocycle and free amine functional groups. However, this radical-polar annulation reaction (RPARs) protocol is highly comfortable with those substrates (Lewis basic heterocycles and free amines substrates). α-Heteroatom, secondary, tertiary and benzylic radical generated from trifluoroborate reagents all smoothly delivered cyclopropanation derivatives [5].

In successive work, the reaction between *bis*(catecholato)alkylsilicates and exocyclic homoallylic tosylates in the presence of photocatalyst 4CzIPN under blue LEDs irradiation afforded polycyclic cyclopropanes (**Figure** 7) [6]. This reaction proceeds smoothly with five (indanone) and six-membered (tetralone) carbocylic tosylate alkenes. But, seven-membered *i.e.* cycloheptanone-based tosylate failed to provide a cyclopropanation product. However, the introduction of heteroatoms (nitrogen and oxygen) in the benzylic position of seven-membered ring *i.e.* benzoazepines and

benzoxepines-derivatives, smoothly afforded Radical-Polar Crossover (RAC) annulation products (**Figure 7**) [6].

Around the same time, Noble and Aggarwal's group jointly documented 4CzIPN-catalyzed cyclopropane reaction by treating aliphatic carboxylic acids with electron-deficient internal and external chloro alkenes (**Figure 8**) [7]. The reaction proceeded *via* decarboxylative radical addition followed by a polar cyclization cascade pathway (**Figure 8**). This methodology shows broad substrate scope for both acids (including cyclic, acyclic carboxylic acids, amino acids and dipeptides) and electron-withdrawing groups (carboxylate esters, nitriles, primary amides, sulfones and phosphonate esters) attached chloro alkenes.

Homoallyl chlorides provided good yields of 1,1-disubstituted cyclopropanes. On the other hand, allyl chlorides lead to vicinal substituted cyclopropanes with moderate yields. The slightly lowered yield obtained is due to the formation of an allylic ester by-product *via* S_N2 reaction between allylic chloride and carboxylate (**Figure 8**) [7]. It is noteworthy to mention that, this mild organic photocatalyst protocol is applied for the late-stage cyclopropylation of a variety of acid-containing bioactive natural products namely, dehydroabietic acid (terpenes), biotin (vitamin B7), trolox (vitamin E analogue), cholic acid (bile acid) and gemfibrozil (fibrate drug) (**Figure 8**) [7].

From a mechanistic perspective, the excited photocatalyst 4CzIPN* underwent SET with the carboxylate to form a carbon center radical by reduction of the excited photocatalyst to radical anion (4CzIPN·⁻). The carbon center radical underwent Giese-type addition into the homoallyl chloride to generate the stabilized alkyl radical. This stabilized alkyl radical accept a single electron from 4CzIPN·⁻ leading to a stabilized carbanion. Polar 3-exotet cyclization of stabilized carbanion afforded cyclopropane product (**Figure 9**) [7].

The above cyclopropanation reactions have considerable advantages over other reagents such as diazomethane (respiratory irritant) and highly pyrophoric diethylzinc $(C_2H_5)_2Zn$, used in the Simmons-Smith reaction.
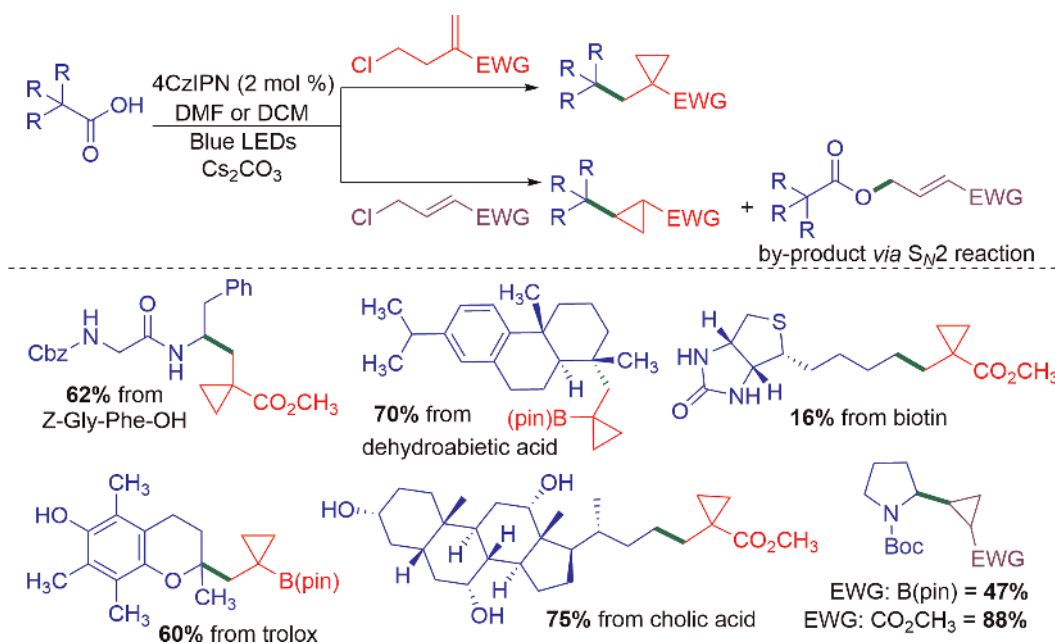

Figure 8.
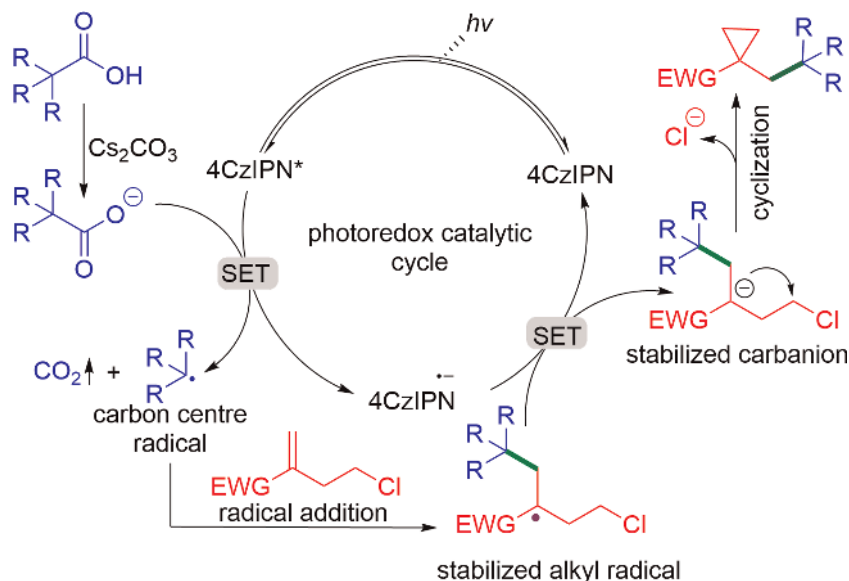*4CzIPN-catalyzed cyclopropanation of allyl and homo allyl chlorides with carboxylic acid.*

Figure 9.
A mechanism for 4CzIPN-catalyzed decarboxylative cascade radical addition–polar cyclization reaction towards substituted cyclopropanes synthesis.

Subsequently, various research groups generated 4CzIPN photo catalyzed decarboxylative carbon-centered radicals from a carboxylic acid and added it into alkenes (*via* Giese-type addition) [8–11] or aromatic heterocyclic (Minisci reaction) [12, 13].

For example, Wang group generated a carbon-centered radical (**10B**) *in-situ via* a decarboxylative path from the anionic form of diethoxyacetic acid (**10A**) by photoirradiation of 4CzIPN. The generated radical (**10B**) adds regioselectively into aryl olefins (styrene derivatives), at the less substituted site which leads to a stable benzylic radical (**10C**). This benzyl radical then accepts a single electron from the radical anion of photocatalyst 4CzIPN·⁻ to form a benzyl anion (**10D**). Protonation of benzyl anion followed by acid hydrolysis of the acetal provided hydroformylation product (**10E**) (**Figure 10**) [8]. In sum, Wang group developed a 4CzIPN catalyzed hydroformylation of aryl olefins with diethoxyacetic (**Figure 10**). In this reaction, diethoxyacetic acid acts as the formylation reagent (formyl radical equivalent). It is noteworthy to mention that this is the first radical-based hydroformylation strategy. The author avoided competitive radical polymerization reaction by performing the reaction in a continuous flow system for electron-deficient olefins, and batch method applied for electron neutral and rich olefinic systems. This radical formylation protocol was successfully extended towards late-stage formylation of biologically relevant complex olefins (**Figure 10**) [8].

The authors studied the competitive reaction between aryl and alkyl olefin in both inter and intra-molecular manners. The reaction showed higher chemoselective at the aryl olefin site. Alkyl olefin site remains intact in both continuous flow and batch method (**Figure 11**) [8].

Schubert group employed 4CzIPN-mediated decarboxylative radical conjugate addition to C=C bonds of dehydroalanine (Dha) and its derivatives peptides (**Figure 12**) [9]. This protocol opens up new avenues to a diastereoselective synthesis of unnatural amino acids and the late-stage derivatization of a tripeptide (**Figure 12**) [9].
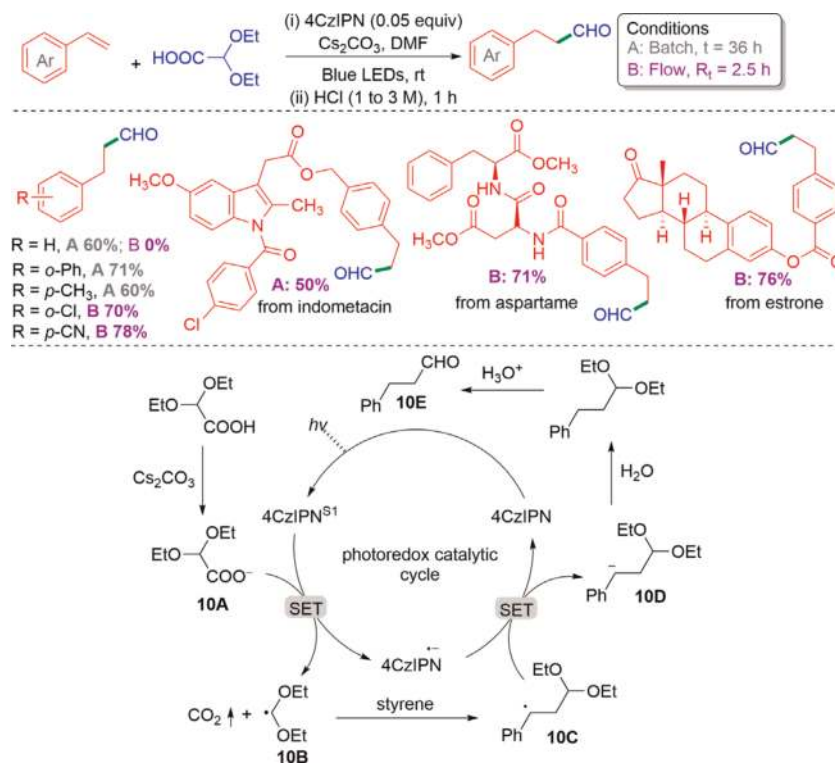
Figure 10.
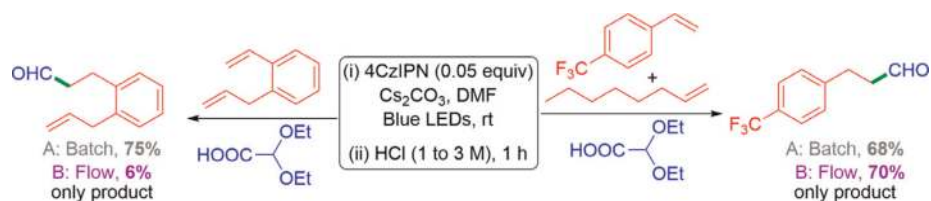*4CzIPN-photoredox catalyzed hydroformylation of olefins.*

Figure 11.
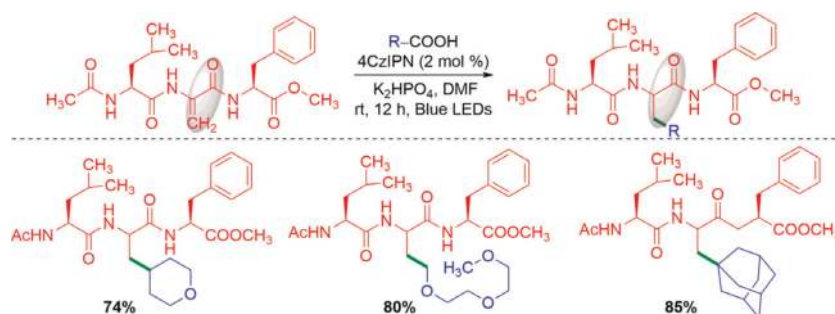*4CzIPN-catalyzed intra- and intermolecular chemoselectivity hydroformylation reactions.*

Figure 12.
4CzIPN-catalyzed radical conjugate addition to dehydroalanine containing tripeptides.

9

3. Three-component C—C and C—N bond formation reaction

So far, we discussed 4CzIPN catalyzed two compound reactions [3–9]. For the first time in the year 2019, the Studer group developed a 4CzIPN photocatalyzed three-component reaction for 1,2-amidoalkynylation of unactivated alkenes (**Figure 13**) [10]. Photoexcited TADF (4CzIPN*) generated an amidyl radical (**14B**) *in-situ* from the anionic form of Troc-protected α-amido-oxy acid (**14A**) *via* a single electron transfer followed by decarboxylation and extrusion of acetone (**Figure 14**). An amidyl radical (**14B**) is added into alkene, which generated an alkyl radical (**14C**), which then couples with an alkyne radical produced from ethynyl benziodoxolones (EBX) to form 1,2-amidoalkynylation product (**14D**) [10].

This three-component reaction showed broad substrate scope for mono, di and tri substituted terminal alkene and substituted benziodoxolones. In addition to these, vinyl ethers, esters and enamides are also compatible with these reaction conditions (**Figure 13**). The reaction provided a high level of chemo-selective product. The polar effect plays a major role in chemo-selective product formation. An amidyl radical is attached at the less substituted site of alkene and the alkyne radical is attached at the more substituted site of alkene (**Figure 13**) [10]. For a particular note, this is the first
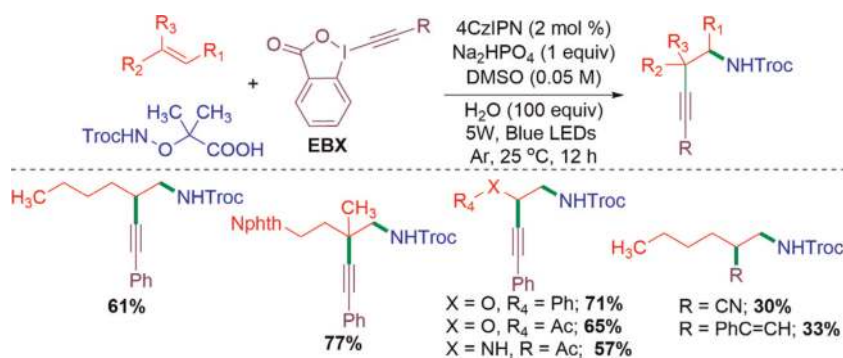

Figure 13.
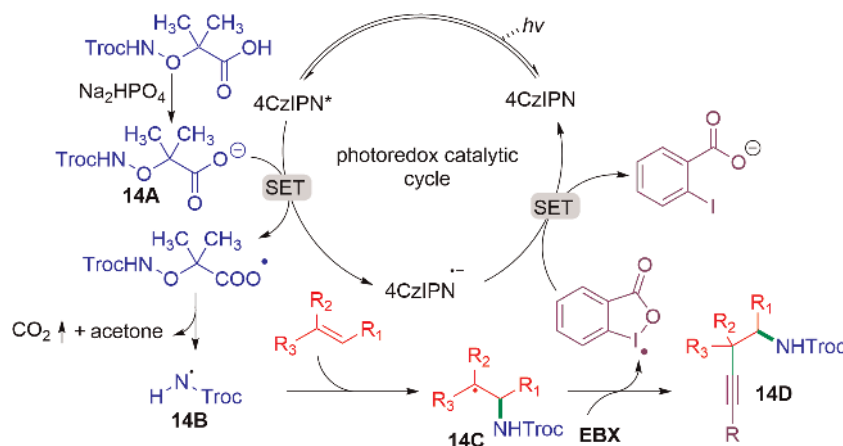*4CzIPN-catalyzed 1,2-amidoalkynylation of unactivated alkenes.*

Figure 14.
Proposed mechanism of 4CzIPN-catalyzed 1,2-amidoalkynylation of unactivated alkenes.

Figure 15.
Radical clock experiments in the synthesis of 1,2-amidoalkynylation of unactivated alkenes.

transition metal-free alkene aminoalkynylation. Before this report, alkene aminoalkynylation reactions are restricted to disubstituted alkenes.

The author concluded that the reaction proceeded through a radical pathway by performing two different radical clock experiments using 1,6-diene and vinylcyclopropane (**Figure 15**) [10].

4. Photoinduced C—Si bond formation via decarboxylation of silacarboxylic acids

All the aforementioned examples deal with photoinduced C—C bond formation *via* decarboxylation of carboxylic acids. In 2020, Uchiyama group generated a silyl radical by photoirradiation of silacarboxylic acids in the presence of 4CzIPN. This silyl radical is successfully trapped by an alkene, leading to silyl alkane *via* C—Si bond formation (**Figure 16**) [11]. Substrate scopes of the reaction were demonstrated with three silacarboxylic acids (Ph$_2$MeSiCOOH, Ph$_2$^{t}BuSiCOOH and PhMe$_2$SiCOOH) and a broad range of electron-withdrawing substituted alkenes (**Figure 16**). Interestingly, 1,1,2,2-tetraphenyldisilane-1-carboxylic acid, (having Si—H and Si—COOH) also provided decarboxylative silyl radical coupled product, without affecting the Si—H group. (**Figure 16**, product no. 16.8) [11].
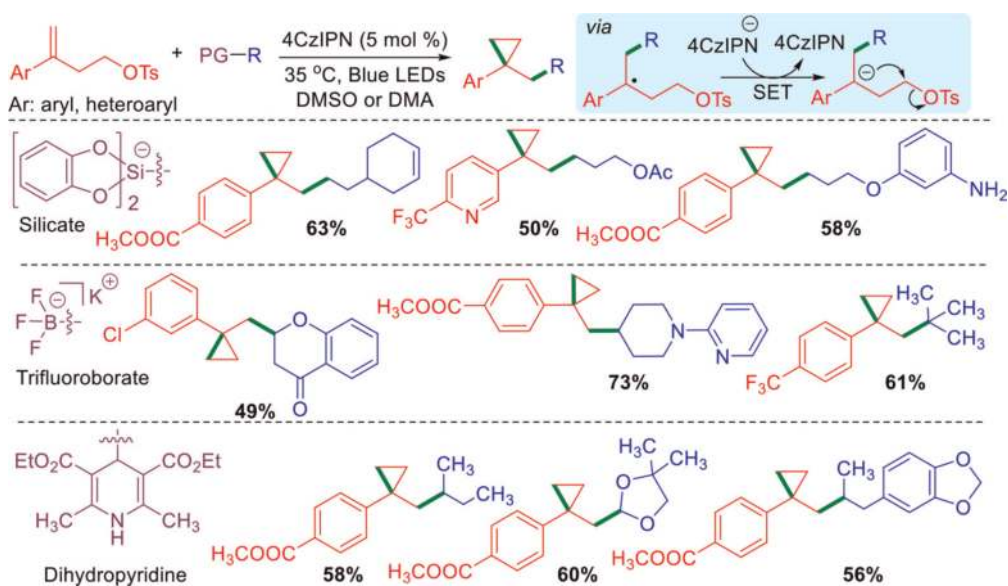

Figure 16.
4CzIPN-catalyzed decarboxylative hydrosilylation of alkenes from silacarboxylic acids.

5. TADF-photocatalyzed Minisci reactions

The addition of nucleophilic radical to electron-deficient nitrogen-containing heteroarenes bases followed by a formal hydrogen atom loss is known as **Minisci reaction** [14, 15]. The major problem associated with the Minisci reaction is regio-selectivity. For example, classical Minisci reaction on quinoline often provides a mixture of C2 and C4 addition products. In 2020, Phipps group developed a TADF-photocatalyzed protocol for regioselective C2 and C4 functionalization of quinoline with phenylalanine-derived redox-active esters (**Figure 17**) [12]. The authors systematically studied the effect of acid, solvents and photocatalyst in the regioselective decarboxylative functionalization (alkylation) of quinolone. The Brønsted acids, photocatalyst and solvent all play major roles in selectivity. The TADF-photocatalyst 4CzIPN with *p*-toluenesulfonic acid (PTSA) in a more polar solvent (DMA) favor C4-functionalized product (5.4:1 ratio of C4/C2). On the other hand, another TADF-photocatalyst 3DPAFIPN with structurally bulky 2,4,6-triisopropylbenzenesulfonic acid (TIPBSA) in a less polar solvent (dioxane) leads to the highest C2 selectivity (C4/C2 = 1:7.3) (**Figure 17**) [12].

Sherwood and co-workers employed a 4CzIPN-photocatalyzed Minisci reaction between a variety of electron-deficient *N*-containing heterocycles and the intermediate of an *in-situ* generated *N*-(acyloxy)phthalimides (NAP) from aliphatic carboxylic acid (**Figure 18**) [13]. Sherwood used various substituted heteroarenes namely
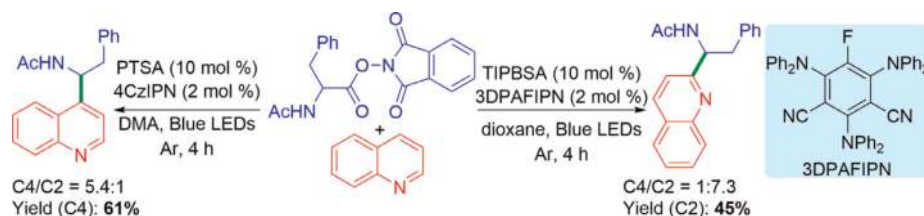

Figure 17.
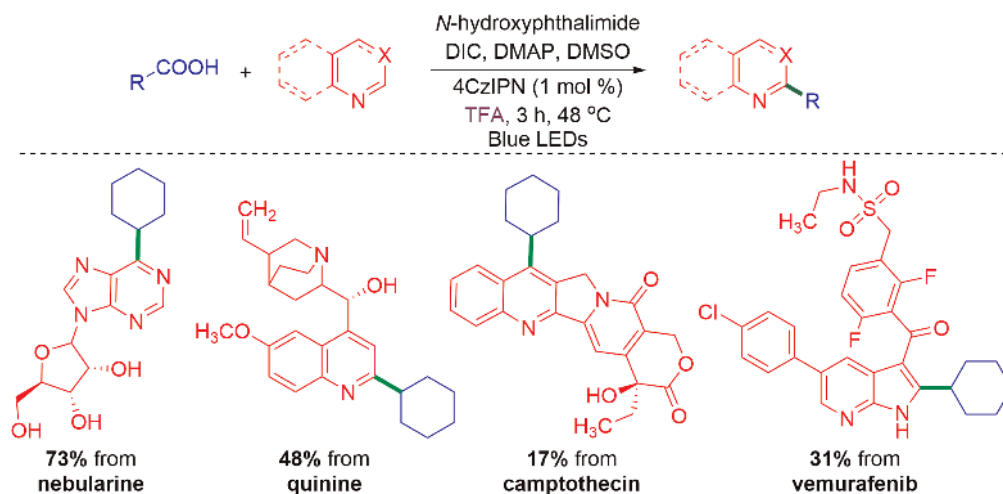*4CzIPN and 3DPAFIPN-photocatalyzed regioselective Minisci reaction of quinoline with redox-active esters.*

Figure 18.
4CzIPN-photocatalyzed one-pot Minisci reaction between hetreoarenes and in-situ generated N-*(acyloxy) phthalimides (NAP).*

pyridine, quinoline, isoquinoline, quinoxaline, quinaldine, quinazolinone, phthalazine, purine, azaindole, benzimidazole, benzothiazole, benzoxazole, indazole and caffeine to test the efficiency of the reaction protocol. Among these, azaindole, benzoxazole and indazole provided the least amount of product (5%), all other substrates afforded moderate to excellent yields of Minisci functionalized products. In addition, this one-pot reaction protocol showed a high degree of functional group tolerance towards late-stage functionalization (LSF) of nucleosides (nebularine and peracetylated nebularine, adenosine), alkaloids (quinine, camptothecin) and anticancer marketed drug scaffolds namely vemurafenib, imatinib (**Figure 18**) [13].

From mechanistic aspects, when blue LEDs light is exposed to organophotocatalyst 4CzIPN and *in-situ* synthesized *N*-(acyloxy)phthalimides (NAP) (**19A**), the latter underwent reductive fragmentation to generate an alkyl radical (**19B**) and phthalimide (by extrusion of carbon dioxide). This is followed by SET from excited 4CzIPN* to a phthaloyl radical. The alkyl radical (**19B**) was added to the electron-deficient *N*-containing protonated heteroarenes (**19C**) to form adducts (**19D**, **E**). The adduct (**19E**) further underwent a second SET with the oxidized form of the organophotocatalyst 4CzIPN·⁺ to give a Minisci product (**19F**) and regenerated the catalyst (**Figure 19**) [13].

In the afore-mentioned Minisci protocols (**Figures 17** and **18**), acid additives were used in the reaction medium [12, 13]. In 2019, Graham and Noonan demonstrated an acid additive-free, large-scale (67 g) photoredox catalyzed Minisci reaction towards the synthesis of 2,4-dichloro-6-[1-(methylsulfanyl)cyclopropyl]pyrimidine (**Figure 20**) [16]. This protocol reduces four reaction steps in the classical production
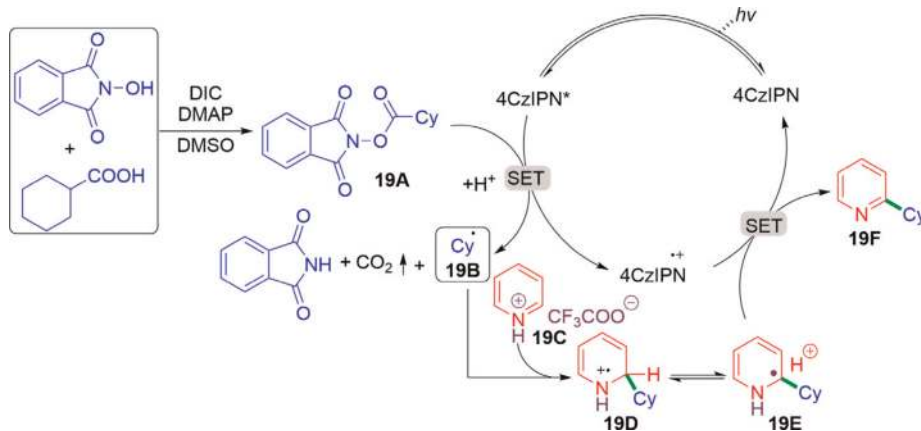

Figure 19.
Proposed mechanism of 4CzIPN-photocatalyzed one-pot Minisci reaction between hetreoarenes and in-situ generated N-*(acyloxy)phthalimides (NAP).*

Figure 20.
3DPA2FBN-photocatalyzed one-pot Minisci reaction towards ceralasrtib synthesis.

Figure 21.
4CzIPN-photocatalyzed decarbonylative Minisci reaction.

of cancer's phase II clinical trials molecule ceralasertib [16]. Compared to 4CzIPN (50% yield), 3-DPA2FBN (70%) is a more effective photocatalyst for the above-mentioned transformation.

In general most of the Minisci reactions proceeds through the decarboxylation ($—CO_2$) pathway [12, 13, 15, 16]. Large amounts of oxidants are generally required when aldehydes are used as the radical precursors. In 2019, Huang and Zhao groups disclosed a visible-light-induced photoredox decarbonylative ($—CO$) Minisci type C—C bond formation (alkylation) between aldehydes and *N*-heteroarenes (**Figure 21**). The reaction proceeded at room temperature and air (O_2) was used as the sole oxidant (**Figure 21**) [17].

This reaction is highly compatible with secondary and tertiary aldehydes. However, primary alkyl aldehydes and aromatic aldehydes failed to deliver decarbonylative Minisci-type alkylated products. The substrate scope of this aerobic photoredox decarbonylative alkylation reaction is decorated by various mono *N*-heteroarenes (quinolines, isonicotinonitrile, isoquinoline, phenanthridine, quinoxyfen, hydroquinine, and benzothiazole) and multi-nitrogen containing heteroarenes such as 1,10-phenanthroline, phthalazine, quinoxaline and imidazo[1,2-a]pyridine. Mono-nitrogen heteroarenes provided a good yield of Minisci-type alkylation products. On the other hand, multi-nitrogen-containing heteroarenes delivered a lower yield of products (**Figure 21**) [17].

The author proposed a plausible reaction mechanism, as shown in **Figure 22**. Visible light-induced photoexcited catalyst 4CzIPN* underwent SET with O_2 to form a superoxide radical anion ($O_2^{\cdot-}$). This superoxide radical anion abstracts a hydrogen atom from aldehyde to produce an acyl radical (**22A**). Decarbonylation of an acyl radical (**22A**) generates an alkyl radical (**22B**). The alkyl radical (**22B**) addition to the protonated *N*-heteroarene (**22C**) leads to *N*-heteroarene radical cation (**22D**). Further, sequential deprotonation of radical cation (**22D**) and SET between alpha alkyl radical and [4CzIPN]⁺ afforded final alkylated quinolone product (**22E**) and regeneration of photocatalyst 4CzIPN (**Figure 22**) [17].

6. Cross-dehydrogenative Minisci type reactions

Cross dehydrogenative coupling (CDC) reaction is step and atom economical reaction. It plays a vital role in the construction of a diverse array of C—C and C—heteroatom bonds, by functionalizing C—H bonds of all types sp, sp^2, sp^3 [18–23].
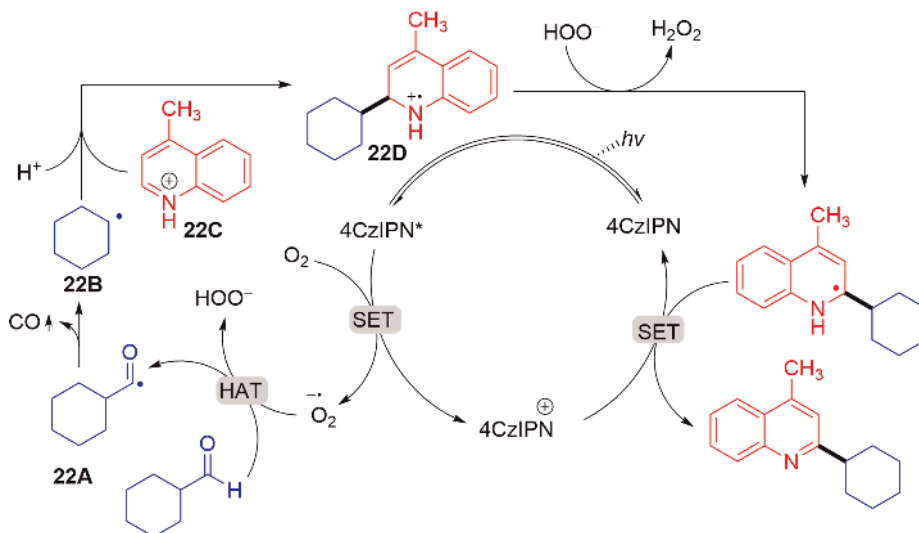
Figure 22.
A plausible mechanism for 4CzIPN-photocatalyzed decarbonylative Minisci reaction.

Figure 23.
A plausible mechanism for 4CzIPN-photocatalyzed decarbonylative Minisci reaction.

In 2020 Li and An group demonstrated an acid-free, 4CzIPN photocatalyzed, Minisci reaction between diverse Csp^3—H sources and *N*-heteroarenes (**Figure 23**) [24].

Sun group developed 4CzIPN and quinuclidine-catalyzed direct C—H silylation of quinoxalinones or electron-deficient heteroarenes *via* Cross Dehydrogenative Coupling (CDC) between quinoxalinones Csp^2—H and silane Si—H bond (**Figure 24**). The reaction proceeded with the combination of photoredox (4CzIPN) and hydrogen atom transfer (HAT) catalyst (quinuclidine) (**Figure 24**) [25]. From a mechanistic perspective, a single electron transfer (SET) between photoexcited catalyst 4CzIPN* and quinuclidine (**24.A**) generates 4CzIPN·⁻ radical anion and quinuclidinium radical cation (**24.B**). The hydrogen atom transfer between silane and quinuclidinium radical cation (**24.B**) produced silyl radical (**24.C**) and protonated quinuclidine (**24.D**). Pyridine base accepts hydrogen from protonated quinuclidine (**24.D**) to regenerate hydrogen atom transfer (HAT) catalyst quinuclidine (**24.A**). Meanwhile, the *in-situ* generated silyl radical couple with the quinoxalinones (**24.E**) to form a radical adduct (**24.F**). Parallelly, superoxide radical anion ($O_2^{·-}$) is formed by another single electron transfer (SET) between 4CzIPN·⁻ and $^1O_2$. Finally, the intermediate **24.F** underwent direct hydrogen atom transfer (HAT) with superoxide radical anion ($O_2^{·-}$) to give the desired CDC silylated product **24.G** (**Figure 24**) [25].
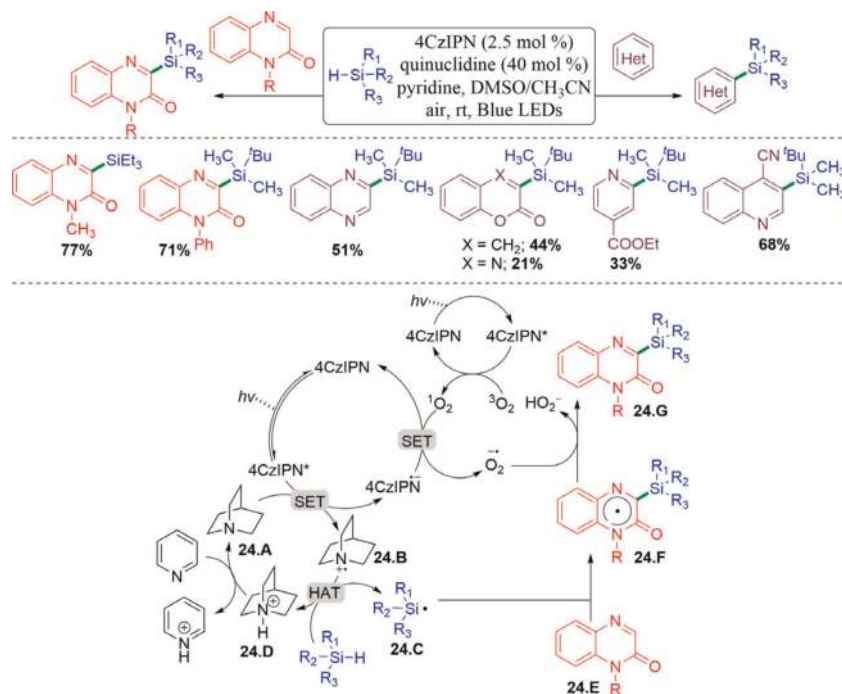
Figure 24.
4CzIPN and quinuclidine catalyzed silylation of quinoxalinones and electron-deficient heteroarenes with alkyl silane via CDC approach.
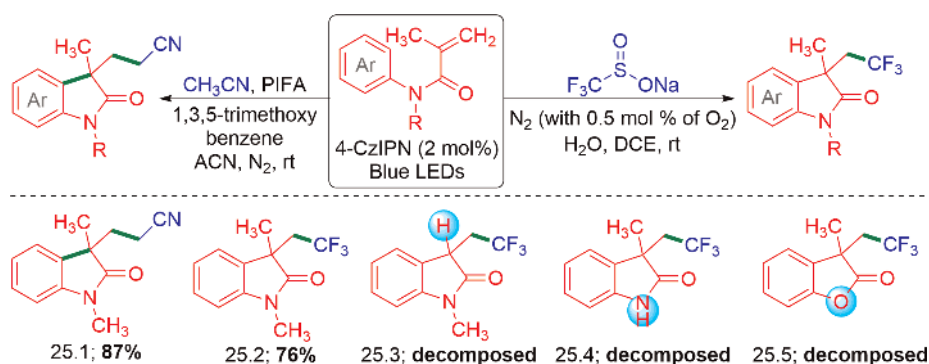

Figure 25.
4CzIPN-photocatalyzed cascade oxidative aryl-trifluoromethylations and aryl-methylcyanation of N-*aryl acrylamides.*

7. Cyclization reactions

Cai group established a 4CzIPN-photocatalyzed intramolecular cascade oxidative aryl-trifluoromethylations [26] and aryl-methylcyanation [27] of *N*-aryl acrylamides for the synthesis of functionalized oxindole (**Figure 25**). Cai used Langlois reagent (sodium triflinate, CF_3SO_2Na) and acetonitrile as trifluoromethyl and methylcyanation sources, respectively. The aryl-trifluoromethylations reaction proceeded without a strong oxidant. Oxygen present in industrial-grade nitrogen (with 0.5 mol% of oxygen) acts as the oxidant. The use of high purity argon (>99.999%) completely failed to provide any trifluoromethylations product (**Figure 25**). On the other hand, aryl-methylcyanation reaction proceeds in the

presence of strong oxidant, phenyliodine *bis*(trifluoroacetate) (PIFA) and an additive 1,3,5-trimethoxybenzene (**Figure 25**). Both aryl-trifluoromethylations [26] and aryl-methylcyanation [27] reactions show broad substrate scope with *N*-aryl, alkyl acryl-amides. However, substrates **25.3**, **25.4** and **25.5** readily decomposed and failed to provide their desired product (**Figure 25**).

From a mechanistic perspective, the photoexcited 4CzIPN* catalyst decomposes sodium triflinate (CF_3SO_2Na) into CF_3 radical and SO_2. This CF_3 radical is added into alkene of *N*-aryl acrylamide to generate a tertiary carbon center radical (**26.A**) or its resonance oxygen radical (**26.B**). Radical cyclization of **26.A** or **26.B** followed by sequential oxidation and deprotonation steps leads to trifluoromethylated oxindole product **26.C** (**Figure 26**) [26].

The author proposed a plausible reaction mechanism of aryl-methylcyanation of *N*-aryl acrylamides, as shown in **Figure 27**. The additive 1,3,5-trimethoxy benzene reacts with phenyliodine *bis*(trifluoroacetate) PIFA to delivered the diaryliodonium salt **27.A**. Which underwent single electron transfer (SET) with excited photocatalyst 4CzIPN*, generated active iodanyl radical **27.B** species. Which abstract acetic hydrogen from acetonitrile or acetone or dimethylsulfoxide to provide the corresponding
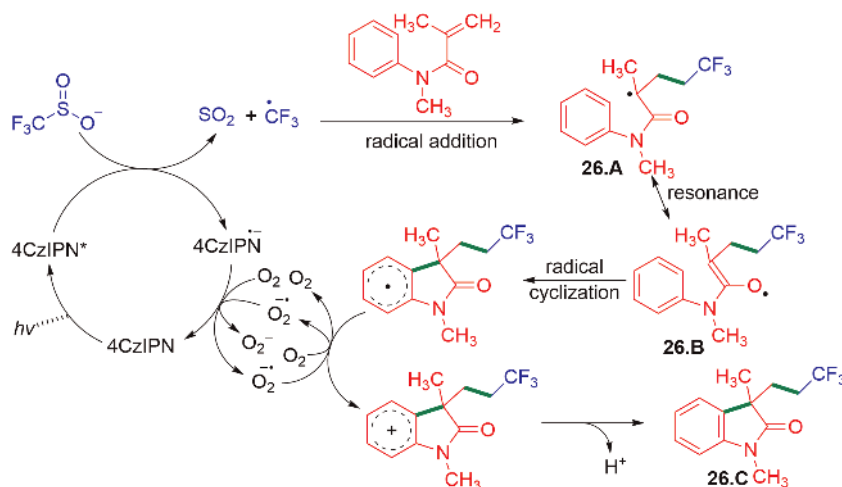

Figure 26.
A plausible mechanism for 4CzIPN-photocatalyzed cascade oxidative aryl-trifluoromethylations and aryl-methylcyanation of N-aryl acrylamides.
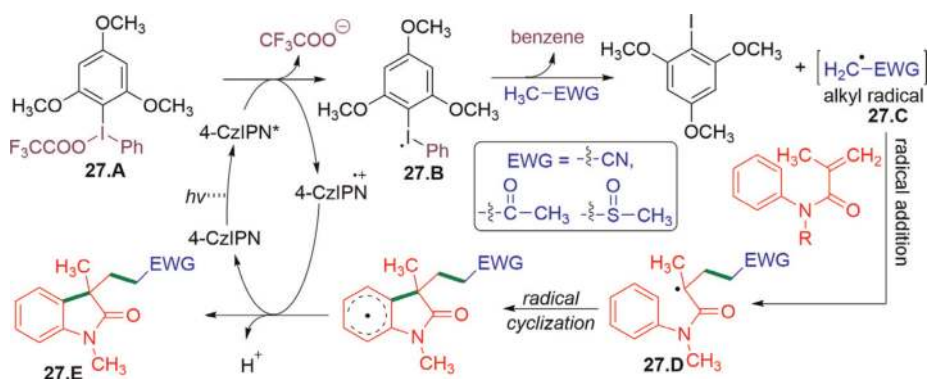

Figure 27.
A plausible mechanism for 4CzIPN-photocatalyzed cascade oxidative aryl-methylcyanation of N-aryl acrylamides.

alkyl radical **27.C**. This alkyl radical underwent radical addition into *N*-aryl acrylamide alkene, which leads to stable tertiary carbon center radical **27.D**. A sequential radical cyclization, followed by deprotonation, afforded alkyl functionalized oxindole product (**27.E**) (**Figure 27**) [27].

Cai group further extended the reaction protocol to *N*-benzoyl acrylamides to synthesize cyano, acetone, dimethylsulfoxide and trifluoromethyl substituted isoquinolinediones (**Figure 28**) [26, 27].

In 2021, Yu group demonstrated a 4CzIPN catalyzed cascade cyclization of *N*-arylpropiolamides to 3-phosphorylated, trifluoromethylated or thiocyanated azaspiro [4.5]trienones (spiro-γ-lactam derivatives). In this radical-initiated cascade annulation reaction, diphenylphosphine oxide or diethyl phosphite, 1-trifluoromethyl-1,2-benziodoxol-3(*1H*)-one (Togni's reagent II) or NH_4SCN have been used as phosphoryl, CF_3 and SCN sources respectively (**Figure 29**) [28]. The reaction showed broad substrate scope for *N*-(4-methoxyphenyl)propiolamides bearing different *N*-substituents (R^1) and Ar substituents (**Figure 29**). Interestingly *N*-arylpropiolamide
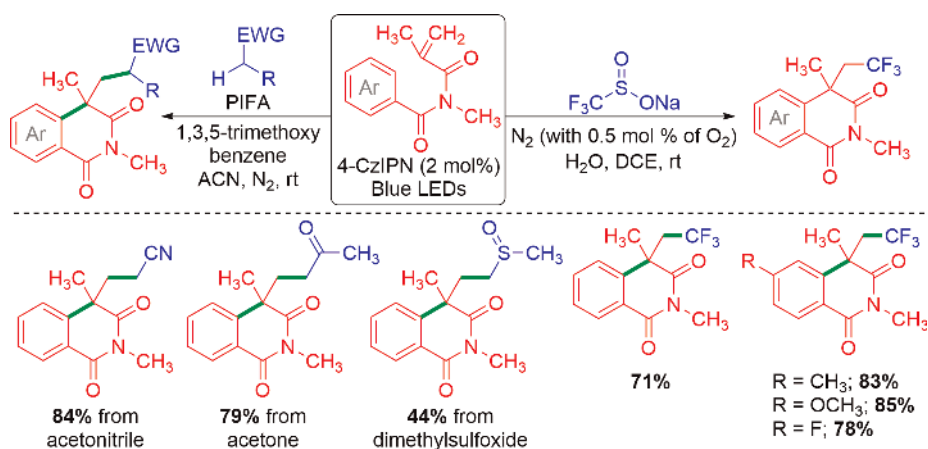

Figure 28.
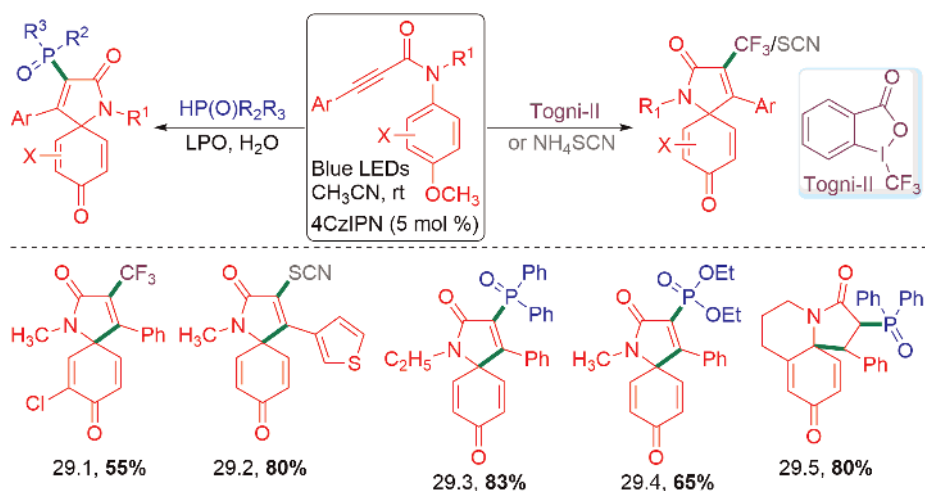*4CzIPN-photocatalyzed cascade oxidative functionalization of* N-*benzoyl acrylamides.*

Figure 29.
4CzIPN-photocatalyzed cascade oxidative functionalization of N-*arylpropiolamides.*
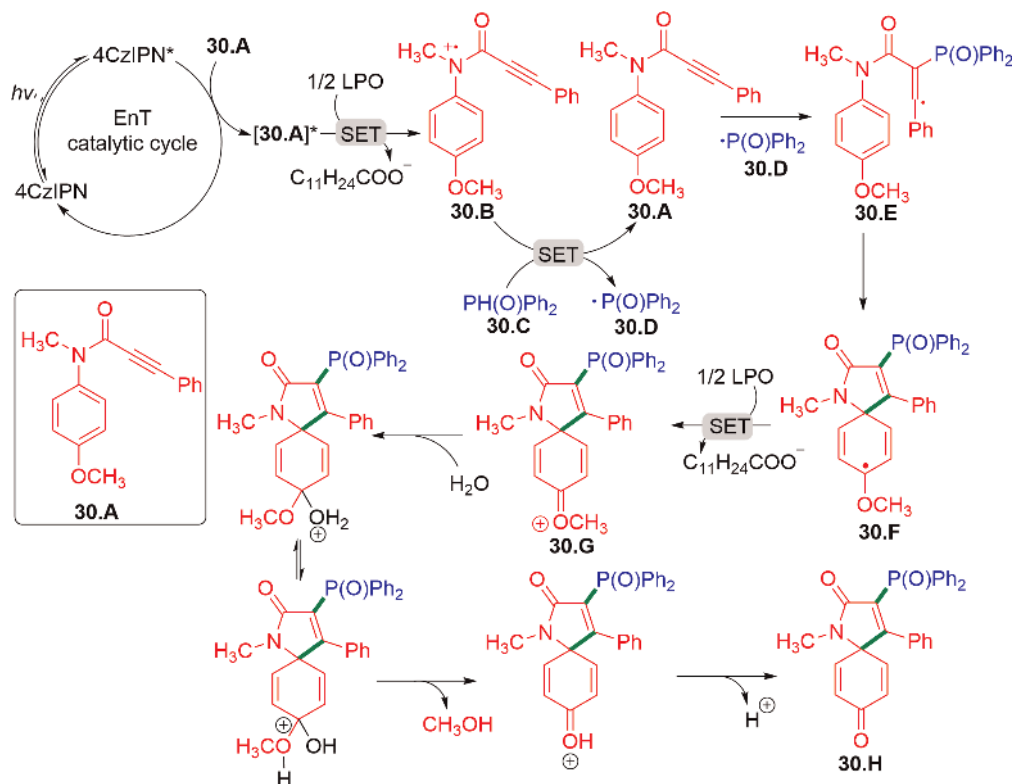
Figure 30.
Proposed mechanism for 4CzIPN-photocatalyzed cascade oxidative functionalization of N-arylpropiolamides.

containing a piperidine ring reacts with diphenylphosphine oxide, providing polyfused heterocycle product **29.5** in very good yield (80%) [28].

This cyclization reaction proceeds *via* the combination of energy transfer (EnT) and single electron transfer (SET) mechanism. The photo-excited catalyst 4CzIPN* transfer its energy to *N*-arylpropiolamide **30.A**, to form a high-energy-level **30.A***. Then a SET between lauroyl peroxide (LPO) and **30.A*** generated *N*-arylpropiolamide radical cation (**30.B**) and dodecanoate anion. Afterward, the second SET between diphenylphosphine oxide (**30.C**) and **30.B** provided *N*-arylpropiolamide **30.A** and diphenylphosphoryl radical (**30.D**). This phosphoryl radical (**30.D**) regioselectively added into alkyne of **30.A**, generated alkenyl radical intermediate (**30.E**). Subsequently it underwent intramolecular radical cyclization to form an azaspiro radical (**30.F**). The third single electron transfer reaction between **30.F** and lauroyl peroxide (LPO) leads to an azaspiro cation (**30.G**) and dodecanoate anion. Sequential addition of H$_2$O, followed by elimination of methanol and deprotonation, provided the desired phosphorylated azaspiro[4.5]trienones product (**30.H**) (**Figure 30**) [28]. A similar reaction mechanism was adopted for trifluromethylated and thiocyanated azaspiro [4.5]trienones synthesis (**Figure 30**) [28].

8. Ring opening reaction

He and co-workers demonstrated a 4CzIPZ catalyzed aerobic oxidative cleavage of unstrained Csp^3—Csp^3 bonds of morpholine derivatives using visible light as the energy source and O$_2$ as an oxidant (**Figure 31**) [29]. The author proposed that the
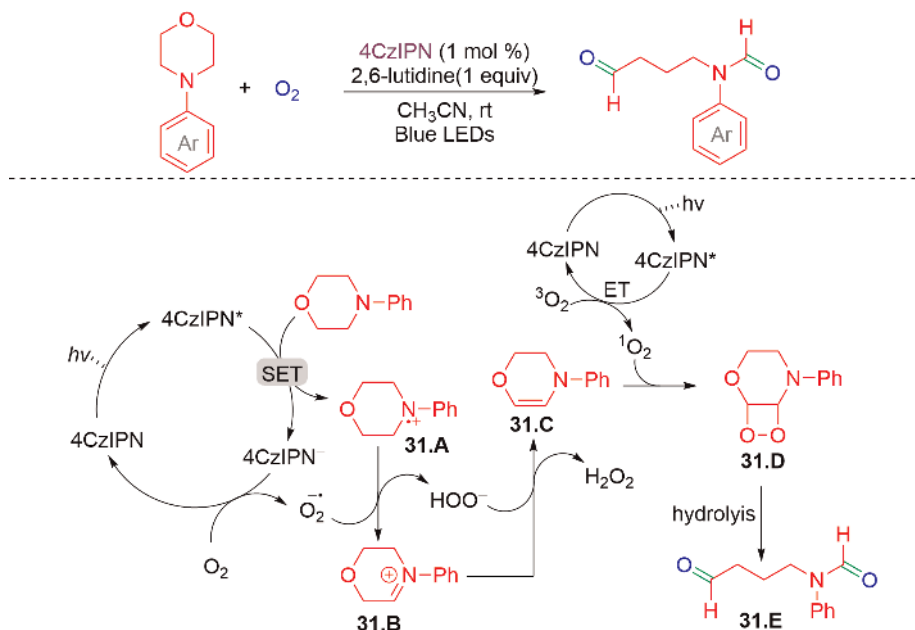
Figure 31.
4CzIPN-photocatalyzed oxidative cleavage of morpholine derivatives.

photoexcited 4CzIPN* was reduced by *N*-aryl morpholine *via* a single electron transfer to generate 4CzIPN⁻ and aminium radical cation (**31.A**). Simultaneously, oxidation of 4CzIPN⁻ by O_2 regenerate photocatalyst 4CzIPN and superoxide anion ($O_2^{\cdot-}$). This superoxide anion ($O_2^{\cdot-}$) abstracts a hydrogen atom from the aminium radical cation (**31.A**) to form an iminium intermediate (**31.B**) and HOO⁻. Afterwards, the HOO⁻ abstracts a proton from the iminium intermediate (**31.B**) and form an enamine species (**31.C**). Concurrently, singlet oxygen ($^1O_2$) is produced by sensitization with 4CzIPN* *via* energy transfer (ET). This singlet oxygen ($^1O_2$) is reacted with enamine (**31.C**) to form a dioxetane intermediate (**31.D**), which readily decompose and provide the desired oxidative cleaved product (**31.E**) [29].

9. Deuteration reaction

In 2020, Leonori and co-workers incorporated deuterium in unactivated 1°, 2° and 3° alkyl iodide using a combination of synergistic photoredox 4CzIPN catalyst and Bu_3N as the halogen atom transfer (XAT)-agent precursor and methyl thioglycolate—D_2O as the D-atom donor (**Figure 32**) [30].

From mechanistic aspects, the excited photocatalyst 4CzIPN* oxidize Bu_3N followed by deprotonation leads to α-aminoalkyl radical (**33.A**) and 4CzIPN$^{\cdot-}$. The α-aminoalkyl radical (**33.A**) abstract a halogen-atom from the alkyl halide to generate an alkyl radical (**33.B**) and α-iodoamine (**33.C**) *via* XAT. This α-iodoamine (**33.C**) species dissociate into the iminium iodide (**33.D**). Meanwhile, HAT, between deuteriated methyl thioglycolate (**33.E**) and alkyl radical (**33.B**) provided desired deuteriated product (**33.F**) and thiol radical (**33.G**). Finally, a single electron transfer between 4CzIPN$^{\cdot-}$ and thiol radical (**33.G**) regenerate photocatalyst 4CzIPN and methyl thioglycolate (**Figure 33**) [30].

In addition to deuteration reaction, Leonori and co-workers further utilized the *in-situ* generated alkyl radical (**34.B**) towards cross-electrophile coupling between
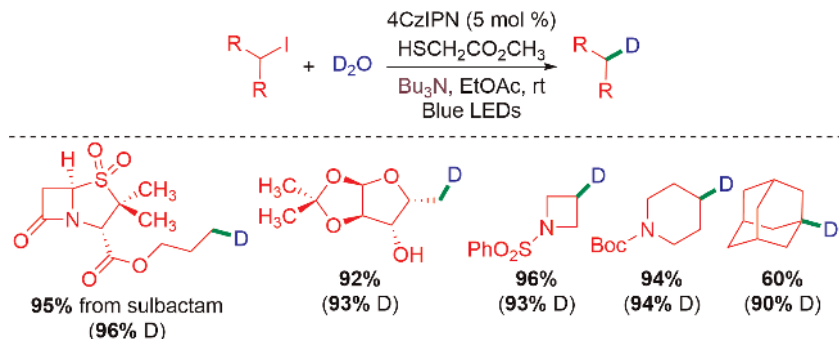
Figure 32.
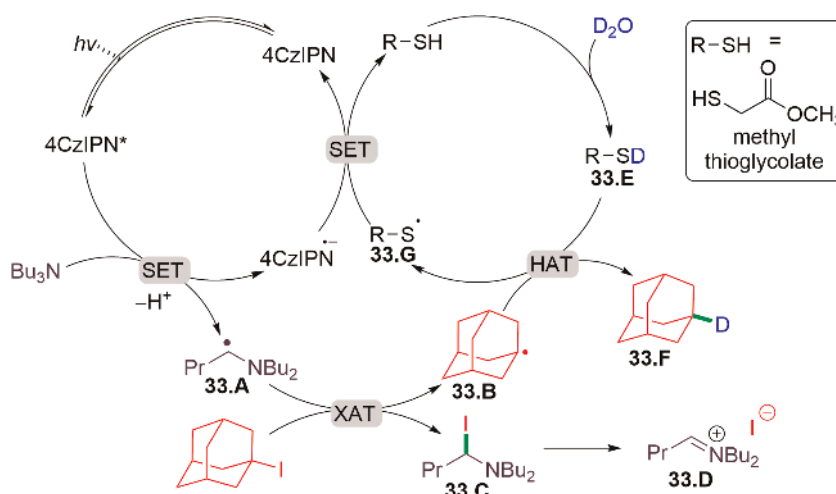*4CzIPN-photocatalyzed deuteration of alkyl halides.*

Figure 33.
Proposed mechanism for 4CzIPN-photocatalyzed deuteration of alkyl halides.
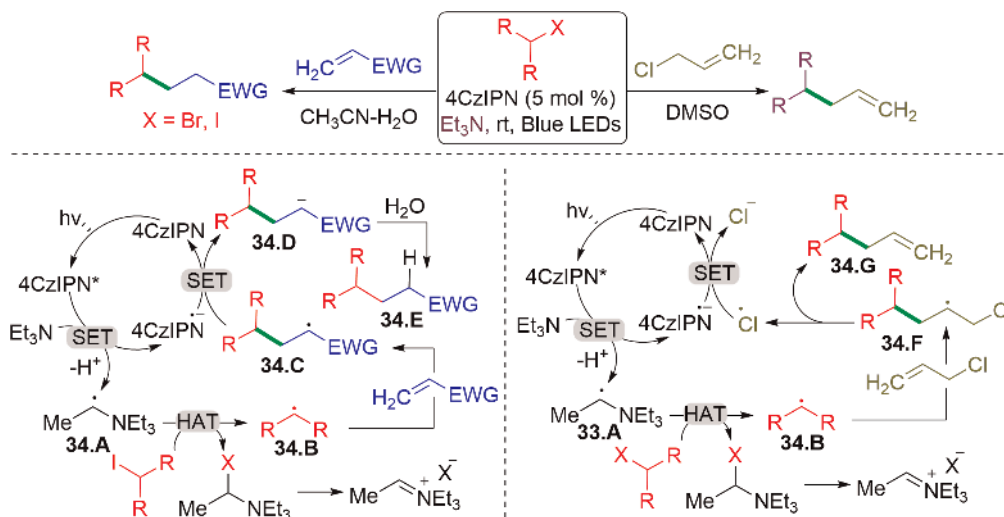
Figure 34.
4CzIPN-photocatalyzed deuteration of alkyl halides. Hydroalkylation and allylation.

electron-deficient olefins or allyl chlorides following Giese-type hydroalkylation mechanism (**Figures 33** and **34**) [30].

10. Conclusions

It is well-known that photocatalytic reactions are powerful tools for a wide range of organic transformations. In this regard, visible-light-induced metal complexes have gained huge attention in the last two decades. Recently TADF materials have been used as an alternative for metal photocatalyst. In this chapter, we summarized a few TADF materials, particularly 4CzIPN as photocatalyst for various radical-based organic transformation reactions. This inexpensive TADF photocatalyst is less toxic and greener. A large number of TADF materials are prepared and used in OLEDs applications. However, only very few TADF molecules are explored in visible light promoted organic transformations. This TADF catalyzed organic transformation reactions are still in its infancy. Many new organo photocatalysts should be discovered for milder organic transformation.

Acknowledgements

Conflict of interest

The authors declare no conflict of interest.

Author details

Suresh Rajamanickam[1,2] and Bhisma K. Patel[1]*

1 Department of Chemistry, Indian Institute of Technology Guwahati, Guwahati, India

2 Materials Research Centre, Indian Institute of Science, Bangalore, Karnataka, India

*Address all correspondence to: patel@iitg.ac.in

IntechOpen

References

[1] Uoyama H, Goushi K, Shizu K, Nomura H, Adachi C. Highly efficient organic light-emitting diodes from delayed fluorescence. Nature. 2012;**492**: 234-238. DOI: 10.1038/nature11687

[2] Wang Y, Carder HM, Wendlandt AE. Synthesis of rare sugar isomers through site-selective epimerization. Nature. 2020;**578**:403-408. DOI: 10.1030/ s41586-020-1937-1

[3] Lévêque C, Chenneberg L, Corcé V, Ollivier C, Fensterbank L. Organic photoredox catalysis for the oxidation of silicates: Applications in radical synthesis and dual catalysis. Chemical Communications. 2016;**52**:9877-9880. DOI: 10.1039/C6CC04636C

[4] Phelan JP, Lang SB, Compton JS, Kelly CB, Dykstra R, Gutierrez O, et al. Redox-neutral photocatalytic cyclopropanation via radical/polar crossover. Journal of the American Chemical Society. 2018;**140**:8037-8047. DOI: 10.1021/jacs.8b05243

[5] Milligan JA, Phelan JP, Polites VC, Kelly CB, Molander GA. Radical/polar annulation reactions (RPARs) enable the modular construction of cyclopropanes. Organic Letters. 2018;**20**:6840-6844. DOI: 10.1021/acs.orglett.8b02968

[6] Milligan JA, Burns KL, Le AV, Polites VC, Wang Z-J, Molander GA, et al. Radical-polar crossover annulation: A platform for accessing polycyclic cyclopropanes. Advanced Synthesis and Catalysis. 2020;**362**:242-247. DOI: 10.1002/adsc.201901051

[7] Shu C, Mega RS, Andreassen BJ, Noble Z, Aggarwal VK. Synthesis of functionalized cyclopropanes from carboxylic acids by a radical addition-polar cyclization cascade. Angewandte Chemie, International Edition. 2018;**57**: 15430-15434. DOI: 10.1002/anie. 201808598

[8] Huang H, Yu C, Zhang Y, Zhang Y, Mariano PS, Wang W. Chemo- and regioselective organo-photoredox catalyzed hydroformylation of styrenes via a radical pathway. Journal of the American Chemical Society. 2017;**139**: 9799-9802. DOI: 10.1021/jacs.7b05082

[9] Zhang O, Schubert JW. Derivatization of amino acids and peptides via photoredox-mediated conjugate addition. The Journal of Organic Chemistry. 2020;**85**:6225-6232. DOI: 10.1021/acs.joc.0c00635

[10] Jiang H, Studer A. Transition-metal-free three-component radical 1,2-amidoalkynylation of unactivated alkenes. Chemistry-A European Journal. 2019;**25**:516-520. DOI: 10.1002/ chem.201805490

[11] Xu N-X, Li B-X, Wang C, Uchiyama M. Sila- and germacarboxylic acids: Precursors for the corresponding silyl and germyl radicals. Angewandte Chemie, International Edition. 2020;**59**: 10639-10644. DOI: 10.1002/anie.2020 03070

[12] Hadrys BW, Phipps RJ. Acid and solvent effects on the regioselectivity of Minisci-type addition to quinolines using amino acid derived redox active esters. Synlett. 2021;**32**:179-184. DOI: 10.1055/s-0040-1707888

[13] Sherwood TC, Li N, Yazdani AN, Dhar TGM. Organocatalyzed, visible-light photoredox-mediated, one-pot Minisci reaction using carboxylic acids via *N*-(acyloxy)phthalimides. The Journal of Organic Chemistry. 2018;**83**:

3000-3012. DOI: 10.1021/acs.joc. 8b00205

[14] Minisci F, Bernardi R, Bertini F, Galli R, Perchinummo M. Nucleophilic character of alkyl radicals-VI: A new convenient selective alkylation of heteroaromatic bases. Tetrahedron. 1971; **27**:3575-3579. DOI: 10.1016/S0040-4020 (01)97768-3

[15] Proctor RSJ, Phipps RJ. Recent advances in Minisci-type reactions. Angewandte Chemie, International Edition. 2019;**58**:13666-13699. DOI: 10.1002/anie.201900977

[16] Graham MA, Noonan G, Cherryman JH, Douglas JJ, Gonzalez M, Jackson LV, et al. Development and proof of concept for a large-scale photoredox additive-free Minisci reaction. Organic Process Research and Development. 2021;**25**:57-67. DOI: 10.1021/acs.oprd.0c00483

[17] Wang Z, Ji X, Zhao J, Huang H. Visible-light-mediated photoredox decarbonylative Minisci-type alkylation with aldehydes under ambient air conditions. Green Chemistry. 2019;**21**: 5512-5516. DOI: 10.1039/c9gc03008e

[18] Rajamanickam S, Saraswat M, Venkataramani S, Patel BK. Intermolecular CDC amination of remote and proximal unactivated Csp^3– H bonds through intrinsic substrate reactivity—expanding towards a traceless directing group. Chemical Science. 2021;**12**:15318-15328. DOI: 10.1039/D1SC04365J

[19] Rajamanickam S, Majji G, Santra SK, Patel BK. Bu_4NI catalyzed C–N bond formation via cross-dehydrogenative coupling of aryl ethers (Csp^3–H) and tetrazoles (N–H). Organic Letters. 2015; **22**:5586-5589. DOI: 10.1021/acs. orglett.5b02749

[20] Mir BA, Banerjee A, Santra SK, Rajamanickam S, Patel BK. Iron(III)-catalyzed peroxide-mediated C-3 functionalization of flavones. Advanced Synthesis and Catalysis. 2016;**358**: 3471-3476. DOI: 10.1002/adsc. 201600565

[21] Majji G, Rout SK, Rajamanickam S, Guin S, Patel BK. Synthesis of esters via sp^3 C-H functionalization. Organic and Biomolecular Chemistry. 2016;**14**: 8178-8211. DOI: 10.1039/C6OB01250G

[22] Majji G, Rajamanickam S, Khatun N, Santra SK, Patel BK. Generation of *bis-*acyl ketals from esters and benzyl amines under oxidative conditions. The Journal of Organic Chemistry. 2015;**80**: 3440-3446. DOI: 10.1021/jo502903d

[23] Rajamanickam S, Sah C, Mir BA, Ghosh S, Sethi G, Yadav V, et al. Bu_4NI-catalyzed, radical-induced regioselective *N*-alkylations and arylations of tetrazoles using organic peroxides/peresters. The Journal of Organic Chemistry. 2020;**85**: 2118-2141. DOI: 10.1021/acs.joc.9b02875

[24] Tian H, Yang H, Tian C, An G, Li G. Cross-dehydrogenative coupling of strong $C(sp^3)$-H with *N*-heteroarenes through visible-light-induced energy transfer. Organic Letters. 2020;**22**: 7709-7715. DOI: 10.1021/acs.orglett. 0c02912

[25] Dai C, Zhan Y, Liu P, Sun P. Organic photoredox catalyzed C-H silylation of quinoxalinones or electron-deficient heteroarenes under ambient air conditions. Green Chemistry. 2021;**23**: 314-319. DOI: 10.1039/D0GC03697H

[26] Lu M, Liu Z, Zhang J, Tian Y, Qin H, Huang M, et al. Synthesis of oxindoles through trifluoromethylation of *N*-aryl acrylamides by photoredox catalysis. Organic and Biomolecular Chemistry.

2018;**16**:6564-6568. DOI: 10.1039/
c8ob01922c

[27] Lu M, Zhang T, Tan D, Chen C,
Zhang Y, Huang M, et al. Visible-light-
promoted oxidative alkylarylation of *N*-
aryl/benzoyl acrylamides through direct
C-H bond functionalization. Advanced
Synthesis and Catalysis. 2019;**361**:
4237-4242. DOI: 10.1002/
adsc.201900712

[28] Zeng F-L, Chen X-L, Sun K, Zhu H-
L, Yuan X-Y, Liu Y, et al. Visible-light-
induced metal-free cascade cyclization
of *N*-arylpropiolamides to 3-
phosphorylated, trifluoromethylated and
thiocyanated azaspiro[4.5]trienones.
Organic Chemistry Frontiers. 2021;**8**:
760-766. DOI: 10.1039/D0QO01410A

[29] Donga C-L, Huanga L-Q, Guana Z,
Huangb C-S, He Y-H. Visible-light-
mediated aerobic oxidative $C(sp^3)$–C
(sp^3) bond cleavage of morpholine
derivatives using 4CzIPN as a
photocatalyst. Advanced Synthesis and
Catalysis. 2021;**363**:3803-3811. DOI:
10.1002/adsc.202100455

[30] Constantin T, Zanini M, Regni A,
Sheikh NS, Julia F, Leonori D.
Aminoalkyl radicals as halogen-atom
transfer agents for activation of alkyl and
aryl halides. Science. 2020;**367**:
1021-1026. DOI: 10.1126/science.
aba2419